

## SUPPORTING INFORMATION

*Verena Fath<sup>1,2</sup>, Stefanie Szmais<sup>3</sup>, Philipp Lau<sup>3</sup>, Norbert Kockmann<sup>1</sup>, Thorsten Röder<sup>2\*</sup>*

### **Model-based Scale-up Predictions: From Micro- to Millireactors using Inline FT-IR Spectroscopy**

<sup>1</sup> Department of Biochemical and Chemical Engineering, Equipment Design, TU Dortmund University, Emil-Figge-Str. 70, 44227 Dortmund/Germany

<sup>2</sup> Institute of Chemical Process Engineering, Mannheim University of Applied Sciences, Paul-Wittsack-Str. 10, 68163 Mannheim/Germany

\*Email address of corresponding author: t.roeder@hs-mannheim.de (Telephone +49 621 292 6800)

<sup>3</sup> Merck KGaA, Frankfurter Str. 250, 64293 Darmstadt/Germany

#### **Table of Contents**

<b>A. Experimental Procedure.....</b>	<b>1</b>
A.1. Reaction .....	1
A.2. Analytical IR spectra and integration method .....	3
A.3. Standard deviations.....	4
<b>B. Mixing.....</b>	<b>7</b>
<b>C. Residence Time Distribution .....</b>	<b>9</b>
<b>D. Heat Removal .....</b>	<b>11</b>
D.1. Temperature tracking during Scale-up experiments.....	11
D.2. Inner heat transfer in case of Kenics static mixers .....	12
D.3. Outside heat transfer .....	15
<b>E. Scale-up Verification.....</b>	<b>18</b>
<b>F. Scale-up Discussion .....</b>	<b>19</b>
<b>Nomenclature.....</b>	<b>20</b>
<b>References .....</b>	<b>21</b>

## A. Experimental Procedure

### A.1. Reaction

Figure S1 displays the titration curve of CH-acidic compound **1** for varying stoichiometric proportions of n-butyllithium. The following experimental parameters were chosen: reaction temperature  $-25\text{ }^{\circ}\text{C}$ , residence time 6 min, initial concentration of CH-acidic compound **1**  $0.8\text{ mol L}^{-1}$ . The total volumetric flow rate was kept constant; only the stoichiometric ratio of n-butyllithium to the CH-acidic compound was varied (through increasing the relative amounts of n-butyllithium within the reaction stream). The high residence time ensures that, under the selected experimental conditions, the reaction of the CH-acidic compound with n-butyllithium always succeeds completely. The resulting IR absorbance of the CH-acidic compound **1** was subsequently tracked.

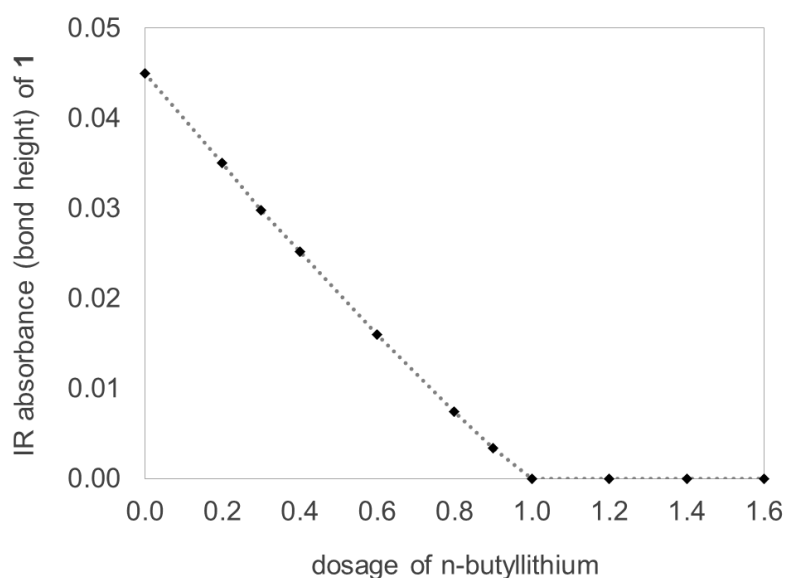


**Figure S1.** Estimation of IR absorbance of CH-acidic compound **1** as function of varying stoichiometric proportions of n-butyllithium.

Thereby, it is demonstrated that the characteristic IR bond of the CH-acidic compound **1** disappears entirely when providing a stoichiometric proportion of n-butyllithium of 1.0. This indicates a 100 % conversion of the CH-acidic compound, which corresponds to the theoretical value that is to be expected for an actual concentration of n-butyllithium amounting to  $1.6\text{ mol L}^{-1}$ , as specified by Sigma Aldrich.

In Figure S2, conversion of CH-acidic compound **1** is plotted against residence time. The experimental data points were obtained in the lab setup at a constant reaction temperature of  $-35\text{ }^{\circ}\text{C}$  and at an initial concentration of CH-acidic compound **1** of  $0.8\text{ mol L}^{-1}$ ; the stoichiometric ratio of n-butyllithium:CH-acidic compound amounted to 0.9. Each experimental series was repeated three times to examine the reaction's reproducibility. All reaction conditions were kept constant, except for the n-butyllithium solution: Three different bottles from different batches were used (one bottle per series, direct dosage from the bottle).

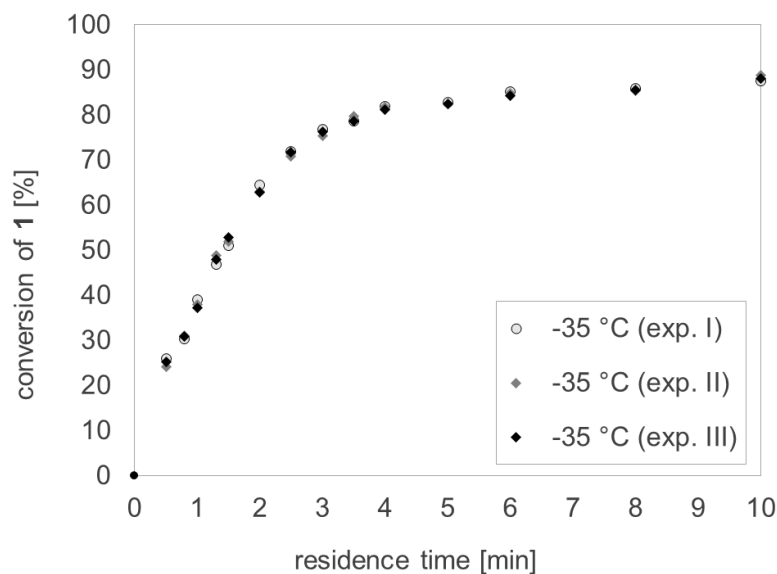


Figure S2. Conversion profile of CH-acidic compound **1** as function of residence time.

Experiments were performed within lab setup at a constant reaction temperature of  $-35\text{ }^{\circ}\text{C}$ , an initial concentration of CH-acidic compound **1** of  $0.8\text{ mol L}^{-1}$ , and a stoichiometric ratio n-BuLi:CH-acidic compound of 0.9. Every experimental data point was repeated three times.

The averaged relative standard deviation of all measured data points (while comparing three different data points at a constant residence time and reaction temperature in each case) amounted to 1 %. Thus, it is demonstrated that the influence of using different bottles of n-butyllithium on the conversion profile is negligible.

## A.2. Analytical IR spectra and integration method

Analytical IR spectra and details on the integration method are exemplarily provided in Figure S3. The evaluation of the characteristic IR bond is based on a calculation of bond height. This is illustrated in Figure S3 for experimental data at residence time 3 min (see decreasing IR bond at  $782\text{--}755\text{ cm}^{-1}$  compared to bond of CH-acidic compound with initial concentration  $0.8\text{ mol L}^{-1}$ ).

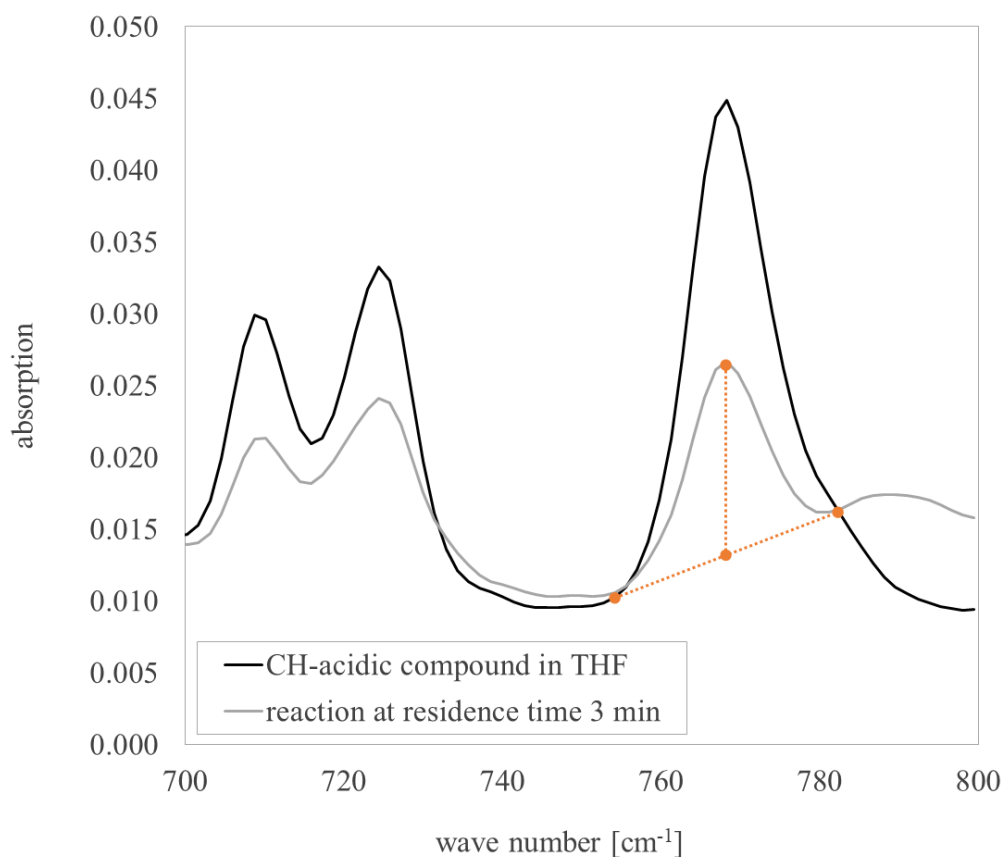


**Figure S3.** Exemplary analytical IR spectra of CH-acidic compound at initial educt concentration of  $0.8\text{ mol L}^{-1}$ , and during reaction with residence time of 3 min (at  $-35\text{ }^{\circ}\text{C}$  and with stoichiometric ratio n-BuLi:CH-acidic compound 0.9).  
Legend: ..... integration method based on calculation of bond height.

### A.3. Standard deviations

The standard deviations after 5 repeated measurements (through inline FT-IR spectroscopy with FlowIR, Mettler Toledo, United States) are provided in Table S1.

**Table S1.** Standard deviations during scale-up experiments (5 repeated measurements).

Reaction temperature	Stoichiometric ratio n-butyllithium:CH-acidic compound	Residence time	Relative standard deviation of IR bond integration at 782–755 cm <sup>-1</sup>
(°C)	(-)	(min)	(%)
-25	0.9	0.3	0.954
		0.4	0.632
		0.5	0.973
		0.8	0.635
		1.0	1.331
		1.3	1.513
		1.5	0.576
		2.0	0.936
		2.5	0.345
		2.5	1.203
		3.0	2.273
		4.0	1.303
-30	0.9	6.0	0.103
		0.3	0.340
		0.4	0.059
		0.5	0.548
		0.8	0.434
		1.0	1.021
		1.3	0.249
		1.5	0.233
		2.0	1.439
		2.5	0.820
		2.5	0.662
		3.0	1.542
4.0	1.490		
6.0	2.368		
8.0	1.869		
10.0	2.404		
-35	0.9	0.3	1.409
		0.4	0.540
		0.5	0.783
		0.8	0.299
		1.0	0.237

		1.3	0.337
		1.5	0.500
		2.0	0.382
		2.5	1.354
		2.5	3.052
		3.0	0.599
		4.0	1.123
		6.0	1.764
		8.0	1.567
		10.0	2.266
-40	0.9	0.3	0.191
		0.4	0.132
		0.5	0.045
		0.8	0.081
		1.0	0.126
		1.3	0.267
		1.5	0.207
		2.0	0.366
		2.5	2.057
		2.5	0.041
		3.0	0.134
		4.0	1.622
		6.0	0.173
		8.0	0.252
		10.0	0.244
-35	0.7	0.3	0.202
		0.4	0.321
		0.5	0.390
		0.8	2.449
		1.0	0.157
		1.3	0.092
		1.5	0.475
		2.0	1.015
		2.5	0.407
		2.5	1.927
		3.0	3.116
		4.0	0.113
		6.0	0.088
		8.0	0.269
		10.0	0.269
-35	0.5	0.3	0.133
		0.4	0.111
		0.5	0.131
		0.8	0.055

---

		1.0	0.106
		1.3	0.116
		1.5	0.282
		2.0	1.158
		2.5	0.299
		2.5	0.112
		3.0	1.026
		4.0	0.285
		6.0	0.412
		8.0	0.307

## B. Mixing

Falk and Commenge<sup>1</sup> developed the stretching efficiency model, which can be used to calculate the theoretical mixing time within a flow channel.

$$t_{\text{mixing, theoretical}} = \frac{(d^2/D_m)}{8 \cdot \text{Pe}} \ln(1.52 \cdot \text{Pe}) \quad (1)$$

The theoretical mixing time can be extended by the energetic efficiency of mixing  $\eta$  to describe real mixing conditions.

$$t_{\text{mixing, real}} = \frac{d}{8 \cdot u \cdot \eta} \ln(1.52 \cdot \text{Pe} \cdot \eta) \quad (2)$$

Figure S4 provides calculated mixing times as function of the Reynolds number  $\text{Re}$ . Thereby, it compares the theoretical mixing time within a flow channel with real mixing times that result when applying several values for energetic efficiency of mixing  $\eta$ .

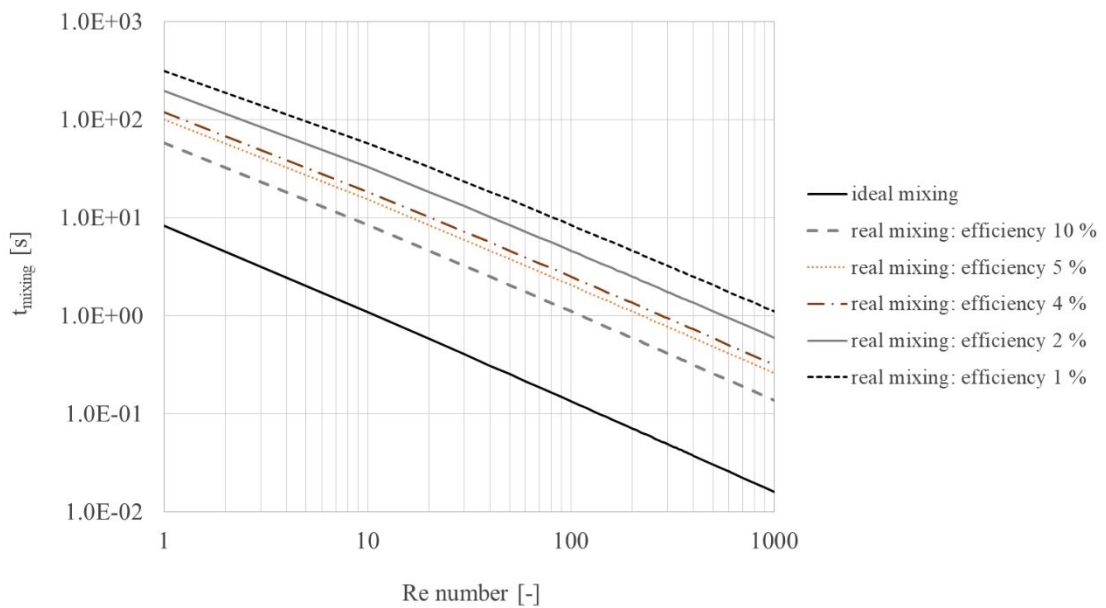


**Figure S4.** Calculated mixing times as function of  $\text{Re}$ . Comparison of theoretical mixing time within a flow channel and real mixing times resulting from different energetic efficiencies of mixing.

It is shown that real mixing times are much longer than the theoretical one. Thereby, real mixing times strongly depend on the value of energetic efficiency of mixing, which can be rather low.

Fang and Lee<sup>2</sup> proposed a correlation for the mixing time in Kenics static mixers as function of Re (valid for  $Re > 150$ ).

$$t_{\text{mixing,Kenics}} = a_i \cdot Re^{-n_{\text{Kenics}}} \quad (3)$$

Two approaches are included: an exponential model (with fitting parameter  $a_1 = 2.21$ ), and a linear model (with fitting parameter  $a_2 = 1.69$ ). The dimensionless parameter  $n_{\text{Kenics}}$  always amounts to 1.5.

Figure S5 compares the two approaches regarding their resulting mixing times, dependent on Re. Mixing times are calculated for Re numbers which were realized during scale-up experiments within the two pilot millireactors.

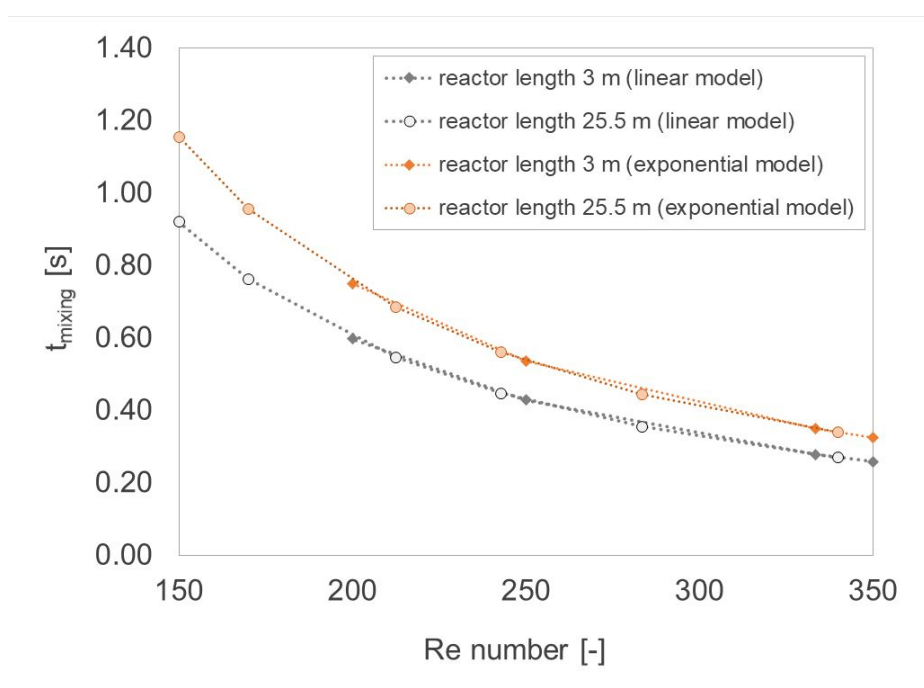


**Figure S5.** Mixing times in Kenics static mixers as function of Re according to Fang and Lee<sup>2</sup>. Two approaches are compared: an exponential model, and a linear model. Legend: mixing times are calculated for Re numbers that were realized within the two pilot millireactors (short reactor: length 3 m, long reactor: length 25.5 m).

Mixing time within a Kenics static mixer (as calculated according to <sup>2</sup>) strongly depends on Re. It should be noted that, for rather low Re numbers  $< 150$ , mixing time can even be higher than 1 s.

### C. Residence Time Distribution

Stimulus-response experiments can be used to estimate residence time behavior within flow channels. Thereby, the extent of axial dispersion can be characterized through the distribution function,  $E(\theta)$ , respectively the cumulative distribution function of residence times,  $F(\theta)$ .<sup>3</sup>

According to Danckwerts<sup>3</sup>, the F-curve (for open boundary conditions, no dispersion discontinuity) can be expressed as:

$$F(\theta) = \frac{1}{2} \left[ 1 - \operatorname{erf} \left( \sqrt{\text{Bo}} \frac{(1 - \theta)}{\sqrt{4 \cdot \theta}} \right) \right] \quad (4)$$

and the E-curve as:

$$E(\theta) = \sqrt{\frac{\text{Bo}}{4 \cdot \pi}} e^{-\frac{\text{Bo}(1 - \theta)^2}{4 \cdot \theta}} \quad (5)$$

Response curves for several flow geometries (plug flow reactor, complete backmixing, micro-lab reactor, pilot millireactor, reactor completely filled with static mixing elements) are provided in Figure S6 and Figure S7.

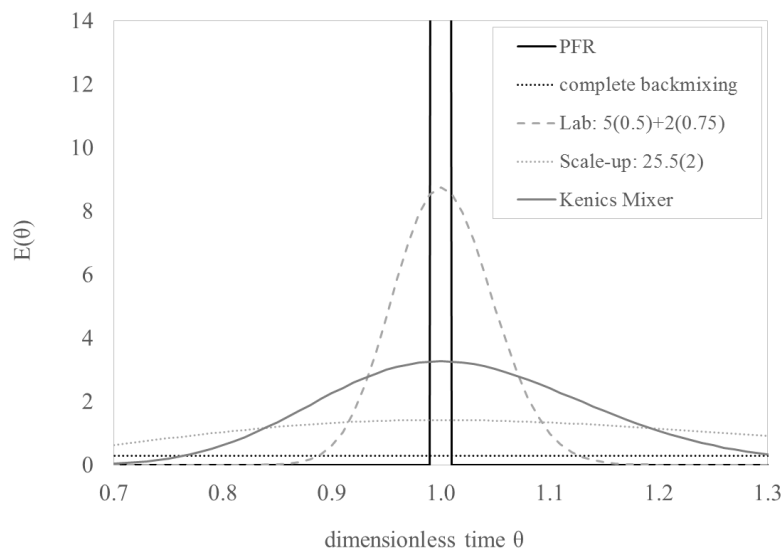


**Figure S6.** E-curve given for several flow geometries.

Legend: Lab reactor – Consisting of two modular reactor pieces that are connected to each other. First capillary: inner diameter 0.5 mm; length 5 m. Second capillary: inner diameter 0.75 mm, length 2 m.

Scale-up – reactor length 25.5 m, inner diameter 2 mm

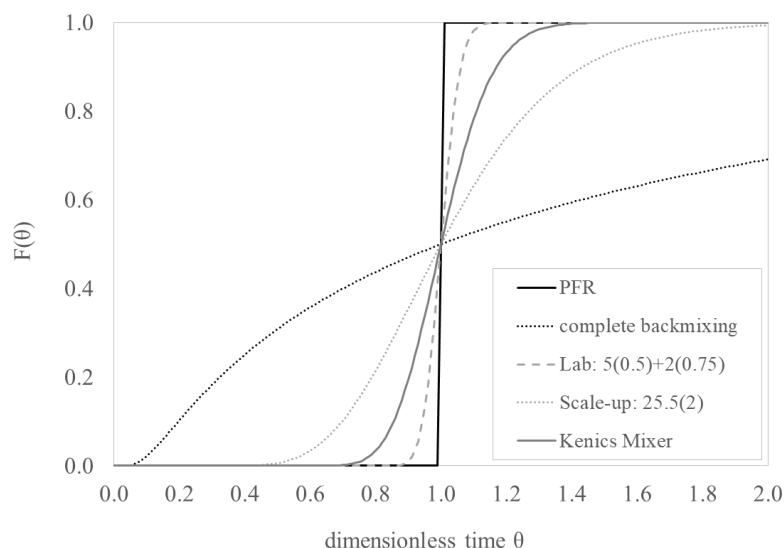


**Figure S7.** F-curve given for several flow geometries.

Comparing the response curves which characterize several flow geometries, it becomes apparent that the pilot millireactor differs more widely from plug flow than the lab reactor. When incorporating Kenics static mixers within the reactor tube, response curves more closely approach plug flow (compared to an empty tube with inner diameter of 2 mm).<sup>4, 5</sup>

Several authors studied residence time behavior when Kenics static mixers are used as reactors, and proposed various models.<sup>6–10</sup> Based on tracer experiments, Brechtelsbauer and Ricard<sup>11</sup> characterized a continuously operating tubular reactor that was completely packed with static mixing elements (intensified plug flow reactor, IPFR). They compared its performance to that of an empty tube, and demonstrated that residence time distribution more closely resembled the one of a plug flow reactor when static mixing elements were used. For all investigated flow rates, corresponding to empty-tube Re numbers between 42 and 167, Bo amounted to values  $> 100$ .

Moreover, the first appearance time  $t_{\text{first}}$  (point in time when the tracer first appears at the reactor outlet) can be used to determine the deviation of a reactor system from plug flow.<sup>4</sup> For a plug flow reactor, the dimensionless first appearance time  $t_{\text{first}}/\bar{t}$  amounts to 1.0, whereas, for an empty pipe with laminar flow, it amounts to 0.5. The closer the value is to 1.0, the lower the effect of backmixing. Based on a model of Nauman<sup>6</sup>, the corresponding value for a 16-element Kenics mixer is 0.598, and 0.676 for a 40-element Kenics mixer. This supports the assumption that the incorporation of Kenics static mixers within a reactor tube reduces axial dispersion.

Nevertheless, it should be noted that, during the scale-up experiments, only a small part of the reactor is filled with static mixing elements. The effect of axial dispersion within the whole pilot reactor can therefore not be fully neglected.

## D. Heat Removal

### D.1. Temperature tracking during Scale-up experiments

In case of the pilot millireactors, temperatures were measured at two stages directly within the reaction stream: after precooling and after the mixer. This allowed for real-time temperature tracking of the reaction process. The temperature after the precooling loop and the one behind the Kenics static mixer are both displayed in Figure S8. A residence time of 2.5 min was realized within both pilot millireactors (the significant difference between their reactor lengths of 3 and 25.5 m required widely varying volumetric flow rates). Hotspot formation among precooling and mixing unit is also included in Figure S8.

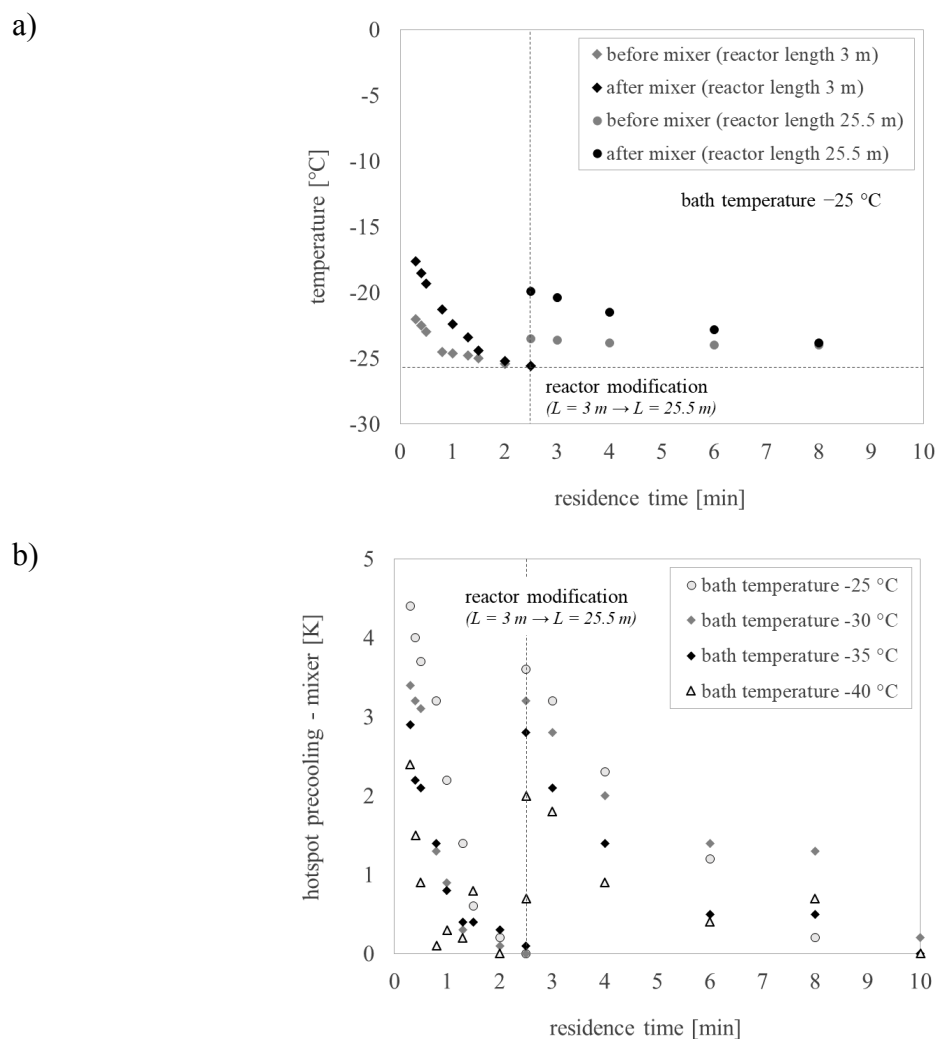


**Figure S8.** Temperature tracking at pilot reactor – hot spot generation between precooling and mixer.

As can be shown in Figure S8, hotspot generation between precooling loop and mixer within the pilot reactors dominates at high mass flows, and runs up to 5 K. When performing the highly exothermic deprotonation reaction at a larger scale, an isothermal state can no longer be assumed.

## D.2. Inner heat transfer in case of Kenics static mixers

In undisturbed laminar flow (empty reactor tubes), heat transfer in radial direction only occurs through thermal diffusion. However, static mixers can be installed, which are thought to increase heat transfer coefficients.<sup>12</sup> Cybulski and Werner<sup>13</sup> proposed a general correlation to predict Nu when static mixers are inserted in pipes.

$$\text{Nu} = \text{Nu}_0 + a' \cdot \text{Re}^{b'} \cdot \text{Pr}^{c'} \cdot \left(\frac{d}{L}\right)^d \quad (6)$$

In this expression,  $\text{Nu}_0$  represents pure thermal conduction ( $\text{Nu}_0 = 3.66$ ).

To estimate Nu as function of Re in tubes containing Kenics static mixers, several correlations derived from the general one are reported in Table S2.

**Table S2.** Correlations for Nu numbers in tubes containing Kenics mixers, as reported in literature.

$\text{Nu} = 6.1 \left( \text{Re} \cdot \text{Pr} \cdot \frac{d}{L} \right)^{\frac{1}{3}} \text{Re}^{-0.71}$	for $\text{Re} < 700$	Joshi et al. <sup>14</sup>
$\text{Nu} = 1.87 (\text{Re} \cdot \text{Pr})^{\frac{1}{3}}$	for laminar regime	Lammers et al. <sup>10</sup>
$\text{Nu} = 3.65 + 3.89 \left( \text{Re} \cdot \text{Pr} \cdot \frac{d}{L} \right)^{\frac{1}{3}}$	for $\text{Re} < 2000$	Grace <sup>15</sup>
$\text{Nu} = 1.44 (\text{Re} \cdot \text{Pr})^{\frac{1}{3}}$	for $\text{Re} < 200$	Cybulski and Werner <sup>13</sup>

$$\text{Nu} = 4.65 \left( \text{Re} \cdot \text{Pr} \cdot \frac{d}{L} \right)^{\frac{1}{3}} \quad \text{for } 200 < \text{Re} < 2000$$

Based on the correlations for heat transfer in Kenics static mixers, Table S3 provides the Nu numbers for lower and upper values of Re. Moreover, heat transfer coefficients were calculated as function of Re (Figure S9).

**Table S3.** Estimated Nu numbers as function of Re, indicated for several Kenics mixer correlations.

	Re = 150	Re = 350
Nu according to Joshi et al. <sup>14</sup>	14	17
Nu according to Lammers et al. <sup>10</sup>	22	29
Nu according to Grace <sup>15</sup>	28	36
Nu according to Cybulski and Werner <sup>13</sup>	17	38

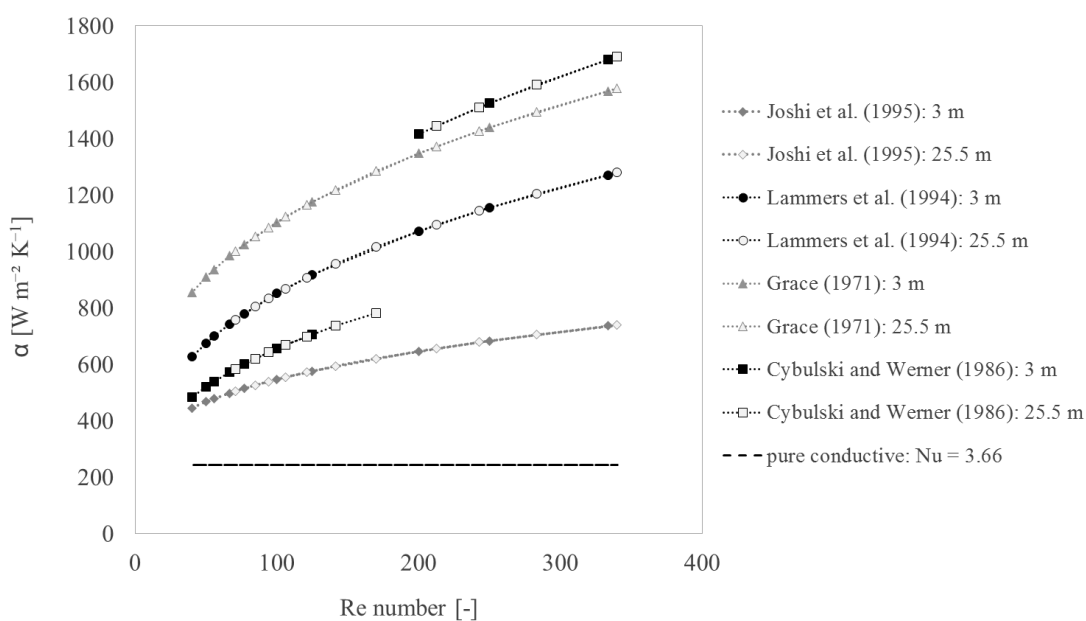


**Figure S9.** Heat transfer coefficients as function of Re, calculated with different correlations for heat transfer within Kenics static mixers.<sup>10, 13–15</sup>

Legend: 3 m – Re numbers realized in short pilot reactor;  
25.5 m – Re numbers realized in long pilot reactor.

In contrast to pure conductive heat transfer with  $Nu = 3.66$ , much higher Nu numbers can be reached once Kenics static mixers are incorporated within reactor tubes. This indicates that Kenics static mixers facilitate heat transfer, and provide faster heat removal compared to empty tubes. However, hotspot generation within the pilot reactors cannot be neglected. This is due to the pilot millireactors not being completely filled with static mixing elements (heat transfer within laminar flow of empty tube is dominating).

It was shown that, compared to an empty tube, the incorporation of Kenics static mixers can foster heat transfer. Several equations for calculating Nu as function of Re were provided in Table S2. Applying them results in several different inner heat transfer coefficients. It should be taken into account that the equations are based on the evaluation of experimental results gained under different specific conditions. Joshi et al.<sup>14</sup> seem to have proposed the most universal correlation (valid for a wide range of Kenics static mixer geometries), and also report the most conservative estimation of improved heat removal. Table S4 outlines the resulting heat transfer coefficients and the differences in maximum temperature increase when applying the described equations (for a coolant temperature of  $-25\text{ }^{\circ}\text{C}$ ).

**Table S4.** Resulting heat transfer coefficients and maximum temperature increases according to several Kenics mixer correlations, as function of Re (coolant temperature  $-25\text{ }^{\circ}\text{C}$ ).

	Re = 150		Re = 350	
	$\alpha$ [W m <sup>-2</sup> K <sup>-1</sup> ]	$\Delta T_{\max}$ [K]	$\alpha$ [W m <sup>-2</sup> K <sup>-1</sup> ]	$\Delta T_{\max}$ [K]
Joshi et al. <sup>14</sup>	602	1	746	0.9
Lammers et al. <sup>10</sup>	975	0.7	1293	0.5
Grace <sup>15</sup>	1240	0.5	1592	0.4
Cybulski and Werner <sup>13</sup>	751	0.9	1708	0.4
Nu = 3.66	245	4	245	4

Compared to pure conductive heat removal with  $Nu = 3.66$  ( $\alpha = 245 \text{ W m}^{-2} \text{ K}^{-1}$ ), which results in a maximum temperature increase of 4 K, all correlations for Kenics static mixers predict much smaller heat releases. Since temperature tracking between precooling and mixer indicates a temperature rise up to 5 K during the exothermic reaction, the application of Kenics static mixer correlations with enhanced heat transfer should be treated carefully. An approach with assuming fully developed laminar flow heat transfer at constant wall temperature ( $Nu = 3.66$ ) proves to be the better choice – especially because only a small area of the reactor tube is filled with static mixing elements (otherwise, the maximum temperature release could be under-estimated).

### D.3. Outside heat transfer

In case of heat transfer through the reactor tube, heat is transferred from the inner reaction fluid to the tube wall by convection, conducted through the wall to the other side, and then transferred to the cooling fluid. Regarding one-dimensional heat transfer, all describes processes are connected in series. Thus, the overall heat resistance can be written as:<sup>16</sup>

$$\frac{1}{U \cdot A_i} = \frac{1}{\alpha_a \cdot A_a} + \frac{s}{\lambda_w \cdot A_m} + \frac{1}{\alpha_i \cdot A_i} \quad (7)$$

As illustrated in eq. 7, the overall heat transfer coefficient  $U$  includes three terms: the inner heat transfer, heat conduction through the reactor tube wall, and the outside heat transfer. Neglect of one of those terms should be considered carefully. Therefore, a discussion of the outside heat transfer is described in the following.

According to Gnielinski<sup>17</sup>, average Nu numbers in cross-flow around single tubes can be calculated using the following correlation:

$$Nu_{l,0} = 0.3 + \sqrt{Nu_{l,lam}^2 + Nu_{l,turb}^2} \quad (8)$$

$$Nu_{l,lam} = 0.664 \cdot \sqrt{Re_l} \cdot \sqrt[3]{Pr} \quad (9)$$

$$Nu_{l,turb} = \frac{0.037 \cdot Re_l^{0.8} \cdot Pr}{1 + 2.443 \cdot Re_l^{-0.1} \cdot \left(Pr^{\frac{2}{3}} - 1\right)} \quad (10)$$

Relevant dimensionless parameters are estimated as follows:

$$\text{Re}_l = \frac{u \cdot l}{\nu} \quad \text{valid for } 10 < \text{Re}_l < 10^7 \quad (11)$$

$$0.6 < \text{Pr} < 1000 \quad (12)$$

$$\text{Nu}_l = \frac{\alpha \cdot l}{\lambda} \quad (13)$$

The streamed length  $l$  (as illustrated in Figure S10) is a function of tube diameter:

$$l = \frac{\pi}{2} \cdot d \quad (14)$$

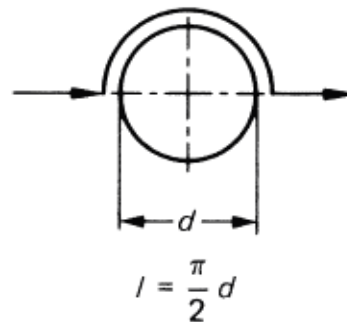


**Figure S10.** Definition of streamed length regarding cross-flow around single tubes.

For cross-flow around rows of tubes, average Nu numbers can be calculated from eq. 8 (cross-flow around single tube) when using the average velocity in the void between the tubes in the row to determine Re. The void fraction  $\psi$  depends on the transverse pitch ratio  $a$  (see Figure S11).

$$a = \frac{s_l}{d_a} \quad (15)$$

$$\psi = 1 - \frac{\pi}{4 \cdot a} = 1 - \frac{\pi \cdot d_a}{4 \cdot s_l} \quad (16)$$

$$\text{Re}_{\psi,l} = \frac{u \cdot l}{\psi \cdot \nu} \quad \text{valid for } 10 < \text{Re}_{\psi,l} < 10^6 \quad (17)$$

$$0.6 < \text{Pr} < 1000 \quad (18)$$

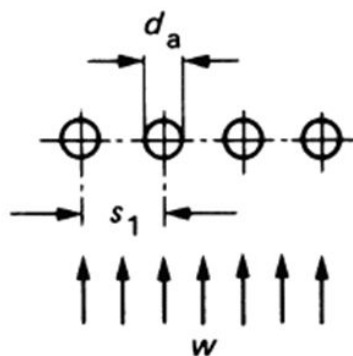


**Figure S11.** Illustration of cross-flow around rows of tubes.

Figure S12 compares resulting heat transfer coefficients when applying the correlations for cross-flow around single tubes and for cross-flow around rows of tubes to pure conductive heat transfer with  $Nu = 3.66 = \text{const}$ . Heat transfer coefficients are provided as function of average flow velocity.

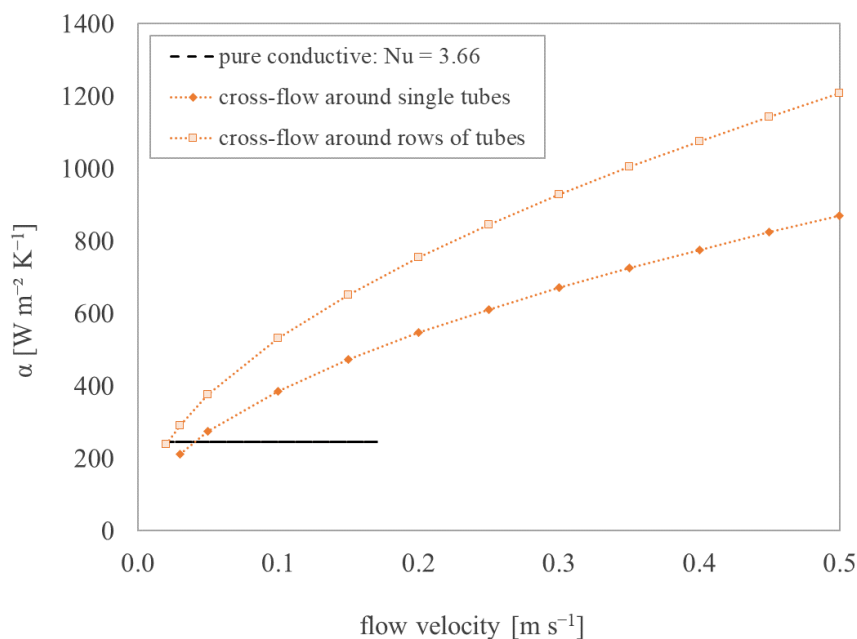
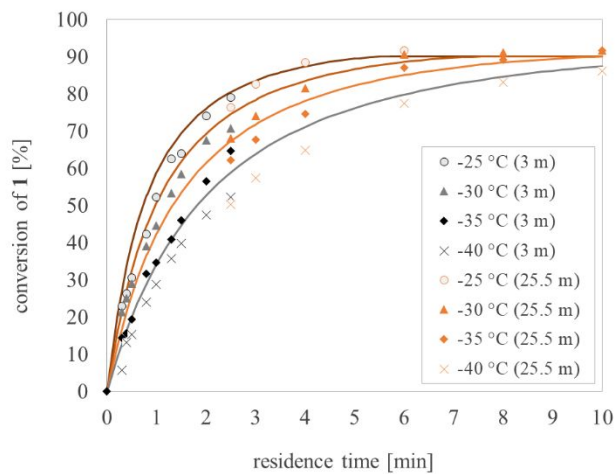


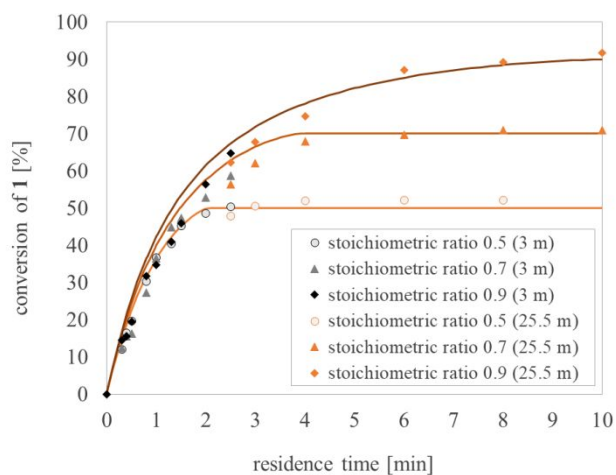
**Figure S12.** Resulting heat transfer coefficients for pure conductive heat transfer, cross-flow around single tubes, and cross-flow around rows of tubes as function of average flow-velocity.

## E. Scale-up Verification

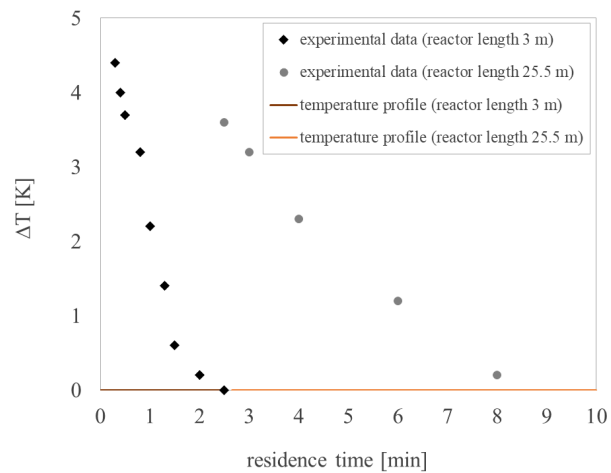
a)



b)



c)



---

**Figure S13.** Simulation of isothermal plug flow reactor compared to experimental data points in pilot reactor. a) Temperature dependence of conversion. b) Influence of varying stoichiometric ratios on educt conversion. c) Reactor outlet temperature at cooling temperature  $-25\text{ }^{\circ}\text{C}$ . Comparison to ideal isothermal model ( $\Delta T = 0\text{ K}$ ). Legend: description of experimental parameters and reactor length (3 m – short pilot reactor; 25.5 m – long pilot reactor).

## F. Scale-up Discussion

Frequencies of squared errors for all experimental data points (concentration profiles) are provided in Figure S14 (for the quick estimate) and in Figure S15 (for the detailed scale-up model). Both figures illustrate how often squared errors appear within defined classes.

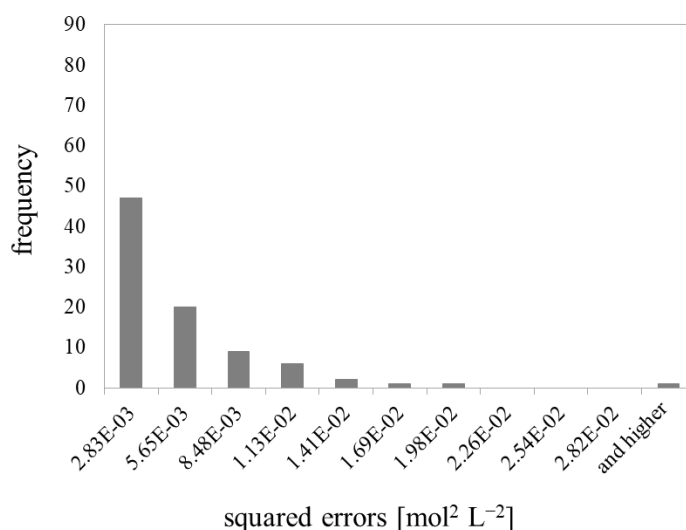


**Figure S14.** Frequency of squared errors of all experimental data points for quick estimate (concentration profiles).

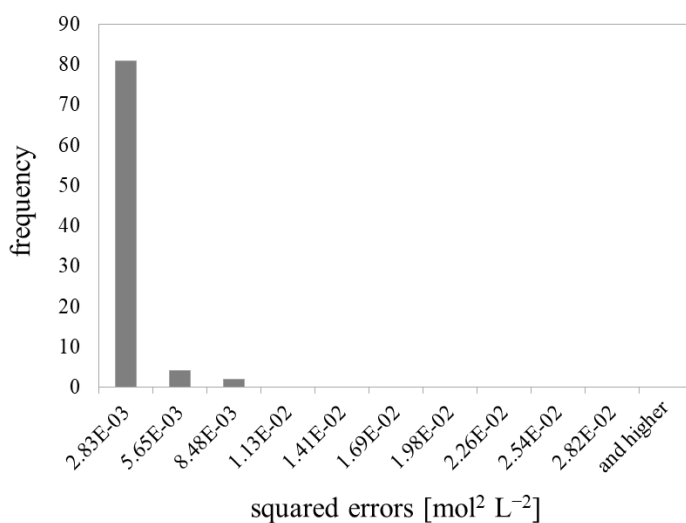


**Figure S15.** Frequency of squared errors of all experimental data points for detailed scale-up model (concentration profiles).

Comparing both scale-up approaches, the detailed model is able to represent the scale-up experiments with higher accuracy since frequency of smallest class of squared errors reaches the highest value.

## Nomenclature

$a$	[-]	transverse pitch ratio
$a_i$	[-]	fitting parameter mixing time Kenics static mixer
$A$	[m <sup>2</sup> ]	area
$Bo$	[-]	Bodenstein number
$d$	[m]	inner capillary diameter
$D_m$	[m <sup>2</sup> s <sup>-1</sup> ]	molecular diffusion coefficient
$E(\theta)$	[-]	distribution function
$F(\theta)$	[-]	cumulative distribution function of residence times
$l$	[m]	characteristic length
$n_{Kenics}$	[-]	dimensionless parameter Kenics static mixer
$Nu$	[-]	Nusselt number
$Pe$	[-]	Peclét number
$Pr$	[-]	Prandtl number
$Re$	[-]	Reynolds number
$s$	[m]	distance
$t_{mixing,Kenics}$	[s]	mixing time in Kenics static mixer
$t_{mixing,real}$	[s]	mixing time under real conditions
$t_{mixing,theoretical}$	[s]	theoretical mixing time
$u$	[m s <sup>-1</sup> ]	flow velocity
$U$	[W m <sup>-2</sup> K <sup>-1</sup> ]	overall heat transfer coefficient

## Greek letters.

$\alpha$	[W m <sup>-2</sup> K <sup>-1</sup> ]	heat transfer coefficient
$\eta$	[-]	energetic efficiency of mixing
$\theta$	[-]	dimensionless time
$\lambda$	[W m <sup>-1</sup> K <sup>-1</sup> ]	thermal conductivity
$\nu$	[m <sup>2</sup> s <sup>-1</sup> ]	kinematic viscosity
$\psi$	[-]	void fraction

## References

- (1) L. Falk, J.-M. Commenge, Performance comparison of micromixers, *Chem. Eng. Sci.* **2010**, *65* (1), 405 – 411. DOI: 10.1016/j.ces.2009.05.045.
- (2) J.Z. Fang, D.J. Lee, Micromixing efficiency in static mixer, *Chem. Eng. Sci.* **2001**, *56* (12), 3797 – 3802. DOI: 10.1016/S0009-2509(01)00098-7.
- (3) P. V. Danckwerts, Continuous flow systems. Distribution of residence times, *Chem. Eng. Sci.* **1995**, *50* (24), 3857 – 3866. DOI: 10.1016/0009-2509(96)81811-2.
- (4) R. K. Thakur, C. Vial, K.D.P. Nigam, E. B. Nauman, G. Djelveh, Static Mixers in the Process Industries, *Chem. Eng. Res. Des.* **2003**, *81* (7), 787 – 826. DOI: 10.1205/026387603322302968.
- (5) J. Aubin, D. F. Fletcher, C. Xuereb, Design of micromixers using CFD modelling, *Chem. Eng. Sci.* **2005**, *60* (8-9), 2503 – 2516. DOI: 10.1016/j.ces.2004.11.043.
- (6) E. B. Nauman, Reactions and residence time distributions in motionless mixers, *Can. J. Chem. Eng.* **1982**, *60* (1), 136 – 140. DOI: 10.1002/cjce.5450600123.
- (7) K. D. P. Nigam, E. B. Nauman, Residence time distributions of power law fluids in motionless mixers, *Can. J. Chem. Eng.* **1985**, *63* (3), 519 – 521. DOI: 10.1002/cjce.5450630322.
- (8) P. Pustelnik, Investigation of residence time distribution in Kenics static mixers, *Chem. Eng. Proc.* **1986**, *20* (3), 147 – 154. DOI: 10.1016/0255-2701(86)85019-X.
- (9) Z. Kembrowski, P. Pustelnik, Residence time distribution of a power-law fluid in Kenics static mixers, *Chem. Eng. Sci.* **1988**, *43* (3), 473 – 478. DOI: 10.1016/0009-2509(88)87008-8.
- (10) G. Lammers, A. A.C.M. Beenackers, Heat transfer and the continuous production of hydroxypropyl starch in a static mixer reactor, *Chem. Eng. Sci.* **1994**, *49* (24), 5097 – 5107. DOI: 10.1016/0009-2509(94)00292-4.
- (11) C. Brechtelsbauer, F. Ricard, Reaction Engineering Evaluation and Utilization of Static Mixer Technology for the Synthesis of Pharmaceuticals, *Org. Process Res. Dev.* **2001**, *5* (6), 646 – 651. DOI: 10.1021/op010056t.
- (12) A. Ghanem, T. Lemenand, D. Della Valle, H. Peerhossaini, Static mixers, *Chem. Eng. Res. Des.* **2014**, *92* (2), 205 – 228. DOI: 10.1016/j.cherd.2013.07.013.
- (13) A. Cybulksi, K. Werner, Static mixers-criteria for applications and selection, *Int. Chem. Eng.* **1986**, *26* (1), 171 – 180.
- (14) P. Joshi, K.D.P. Nigam, E. Bruce Nauman, The kenics static mixer, *Chem. Eng. J.* **1995**, *59*, 265 – 271. DOI: 10.1016/0923-0467(94)02948-2.
- (15) C. D. Grace, ‘Static mixing’ and heat transfer, *Chem. Proc. Eng.* **1971**, 57 – 59.

- (16) Verein Deutscher Ingenieure, *VDI heat atlas*, Springer, Heidelberg **2010**.
- (17) V. Gnielinski, Zur Wärmeübertragung bei laminarer Rohrströmung und konstanter Wandtemperatur, *Chem. Ing. Tech.* **1989**, *61* (2), 160 – 161.  
DOI: 10.1002/cite.330610216.